Hindawi Publishing Corporation
Science and Technology of Nuclear Installations
Volume 2014, Article ID 964585, 7 pages
http://dx.doi.org/10.1155/2014/964585

Research Article

Experimental and Numerical Study on Pressure Distribution of 90° Elbow for Flow Measurement

Beibei Feng, Shiming Wang, Shengqiang Li, Xingtuan Yang, and Shengyao Jiang

Key Laboratory of Advanced Reactor Engineering and Safety, Ministry of Education, Institute of Nuclear and New Energy Technology, Tsinghua University, Beijing 100084, China

Correspondence should be addressed to Beibei Feng; fengbeibei@tsinghua.edu.cn

Received 4 March 2014; Revised 25 May 2014; Accepted 2 June 2014; Published 3 August 2014

Academic Editor: Iztok Tiselj

Numerical simulation is performed to investigate the pressure distribution of helium gas under high pressure and high temperature for 10 MW High Temperature Gas-Cooled Reactor (HTGR-10). Experimental studies are first conducted on a self-built test system to investigate the static pressure distribution of a 90° elbow and validate the credibility of the computational approach. The 90° elbow is designed and manufactured geometrically the same as HTGR-10. Based on the experimental data, comparison of static pressure of inner wall and outer wall of 90° elbow with numerical results is carried out to verify the numerical approach. With high agreement between experimental results and numerical results of water flowing through 90° elbow, flow characteristics of helium gas under high pressure and high temperature are investigated on the confirmed numerical approach for flow measurement. And wall pressure distribution of eight cross sections of 90° elbow is given in detail to represent the entire region of the elbow.

1. Introduction

During the past decades, High Temperature Gas-Cooled Reactor (HTGR) has gained significant development in China due to its inherent safety and high efficiency of power generation [1, 2]. Using helium gas with good chemical inertia and thermal performance as a cryogen, heat produced by fission reaction in the core of HTGR is transferred to the steam generator [3]. For nuclear security and the calculation of thermal power of reactor, measurement of helium gas flow is vital and necessary [4]. However, most measurement methods for helium gas under high pressure and high temperature are difficult due to the restriction of reactor structure and wicked measuring environment [5, 6]. A novel measuring device based on pressure difference created by centrifugal force between the inside diameter and the outside walls of 90° elbow is proposed for helium gas measurement of HTGR owing to its simplicity, reliability, repeatability, and low cost [7, 8]. The flow measurement method consists basically in determining the pressure difference, then assigning it to the corresponding flow rate, following a previously established characteristic of the elbow flow meter [9]. The advantage of elbow flow meter is the fact that measurement signals might be provided by the existing elbows of the steam generator. On the other hand, elbows would lead to high level of disturbances and require straight pipe before and after the elbow to ensure high measuring accuracy [9]. So, investigation of helium gas characteristics flowing a 90° elbow is vital and the use of computational fluid (CFD) would play a significant role to achieve high accuracy and reliability of elbow flow meter.

Validations of CFD results with wall pressure distribution of a 90° elbow will be performed in this paper. Measurements are carried out on a self-built test system to investigate the influence of water flow on inner wall pressure and outer wall pressure of 90° elbow. With regard to three-dimensional flow structure, disposal of pressure detecting points in axial cross section of pipe is adopted to measure the water flow and compared their CFD pressure predictions with measurements. Through all these experimental and numerical studies, investigation of pressure distribution of helium gas under high temperature and high pressure through 90° elbow has been the primary focus of this paper because wall pressure

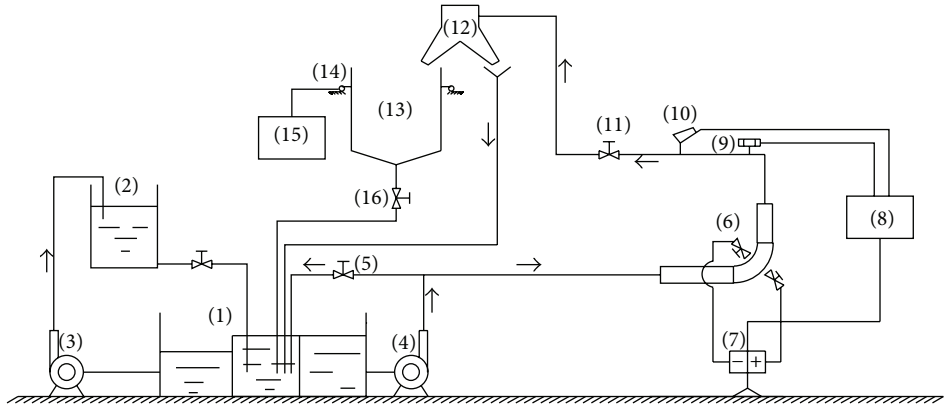

(1) Spilling tank
(2) Water replenishing tank
(3) Supply pump
(4) Main pump
(5) Control valve
(6) Elbow flowmeter
(7) Differential pressure transmitter
(8) Main instrument
(9) Pressure transmitter
(10) Temperature transmitter
(11) Control valve
(12) Commutator
(13) Weighing tank
(14) Weighing sensor
(15) Weighing indicator
(16) Water drain valve

Figure 1: Schematic view of experimental setup for the wall pressure distribution measurement of intrados and extrados of 90° elbow.

distribution of 90° elbow is most relevant to the accuracy of elbow flow meter.

2. Experimental Setup for Pressure Measurement

The experiments were carried out through a self-built water cycle system using fifteen differential pressure transmitters measuring pressure distribution of intrados and extrados of 90° elbow. Figure 1 shows a schematic view of the typical experimental setup. Its basic part is an elbow flow meter with an internal diameter of $D_{in} = 96$ mm, consisting of three parts—a vertical pipe with $L_1 = 1\,\text{m} \approx 10D_{in}$, a 90° elbow with an average radius of $R = 350$ mm, and straight pip section after the elbow with a length of $L_2 = 1\,\text{m} \approx 10D_{in}$. At the inner wall and outer wall of 90° elbow, 15 measuring orifices are arranged with appropriate distance. Flow velocity of test system is adjusted through variable voltage and variable frequency to control the main pump (4). Calibration of flow velocity is carried out through weight method on an additional system composed of weighing tank (13), weighing sensor (14), and weighing indicator and the value of calibrated error is less than 0.05%. Arrangement of pressure taps of 90° elbow is illustrated in Figure 2. We can measure wall pressure distribution of intrados and extrados of 90° elbow through 15 points with several angles (such as 5°, 15°, 22.5°, 35.0°, 45.0°, 53.0°, 58.0°, 70.0°, and 85.0°), respectively. The measurement is performed using the pressure transmitter EJA110A-DLS5A-22NC when flow velocity of water cycle is arranged from $0.5\,\text{m} \cdot \text{s}^{-1}$ to $3.5\,\text{m} \cdot \text{s}^{-1}$ with an interval of $0.5\,\text{m} \cdot \text{s}^{-1}$. The experiments are considered at the Reynolds number range Re = 47000–330000.

3. Numerical Details of the CFD Simulation

Numerical simulation is performed on the 3D virtual model which is identical to the 90° elbow used in pressure measuring experiments. The computational model consists of a horizontal inlet pipe with a length of 10 pipe diameters, a 90° horizontal-placed elbow with a bending diameter ratio (the ratio radius of 90° elbow and pipe diameter) of 1.5, and a horizontal outlet pipe with a length of 15 pipe diameters established referring to the 90° elbow of steam generator, as shown in Figures 3(a) and 3(b).

Experimentally derived inlet velocities are set at the inlet of the CFD model. To minimize the influence of pipe's openings, extended regions are also incorporated at both inlet and outlet of CFD model. As shown in Figure 3(c), a mesh consisting of three-dimensional hexahedral elements is generated via ICEM over the entire flow domain. Grid sensitivity test is carried out at three different grid mesh levels: coarse (61,440 cells), medium (344,064 cells), and fine (884,736 cells). A discrepancy of 0.5% is observed through comparing the predicted maximum dynamic pressure at the specific point on the extrados of 90° elbow between the medium meshes and fine meshes. It can thereby be concluded that the fine mesh can be employed in obtaining grid independent solutions [10]. In order to achieve high accuracy results, the mesh is narrowed especially at places where high gradients of the calculated values occur, that is, close to the walls. The thickness of the smallest element adjacent to the wall is 0.1 mm, and the thickness increase coefficient (quotient of the thickness of the preceding element and the next one) adjacent to the wall is 1.1. Considering that the pressure distribution varies significantly in the elbow flow region, the adaptive grid method is applied to refine the

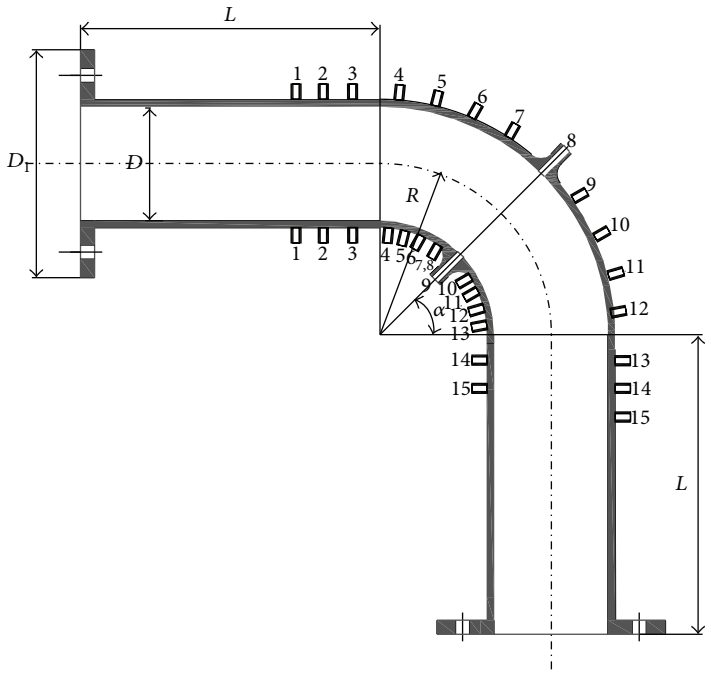

Figure 2: Arrangement of measuring orifices of 90° elbow.

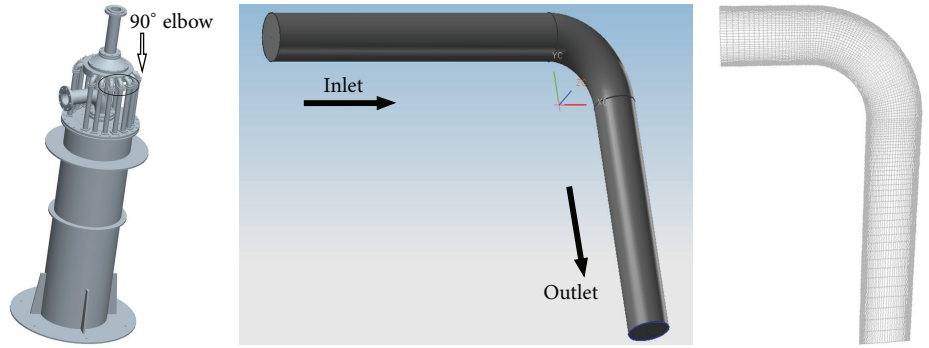

(a) (b) (c)

Figure 3: Three-dimensional views of 90° elbow of steam generator and established CFD model. (a) Structural 90° elbow of steam generator; (b) CFD model; (c) the view of mesh distribution of the axial cross section.

computational domain again to capture more information about the formation and development of the secondary flow. The discrepancy and the grid sensitivity are listed in Table 1. Low levels of discrepancy between coarse mesh and medium mesh show enough fine mesh. Consequently, medium mesh is adopted in numerical calculations considering enough calculation accuracy and efficiency.

The computation is accomplished using a two-equation turbulence model k-ω available in the FLUENT software package. The water flowing 90° elbow is considered to be steady, isothermal, incompressible, and Newtonian. Consistent with the experiment, wall boundaries of CFD model are assumed to be rigid and impermeable. A generic finite volume CFD code FLUENT is utilized to solve the Navier-Stokes equations. Numerical solutions are obtained through the iterative algebraic multigrid solver with the advection terms approximated via the second-order upwind differencing scheme. In the present study, reliable convergence is achieved within 3000 iterations when the RMS (root mean square) pressure residual dropped below 1.0×10^{-7}.

4. Results

4.1. Comparison between Experimental and Numerical Results. The experiments are carried out through a self-built water cycle system using 15 differential pressure transmitters measuring pressure distribution of intrados and extrados of 90° elbow. Numerical results are obtained with the assistance of the FLUENT software package. Figure 4 presents the comparison of measured static pressure profile with the numerical results for flow velocities 0.5 m/s, 1.5 m/s, and 2.5 m/s, respectively. Equivalent points in the figures are used

Table 1: Grid sensitivity between coarse mesh and medium mesh.

Wall pressure		Static pressure/Pa		Dynamic pressure/Pa	
		Min	Max	Min	Max
Coarse mesh	61440	6998029	7001147	230	4023
Medium mesh	344064	6998053	7001164	242	4072

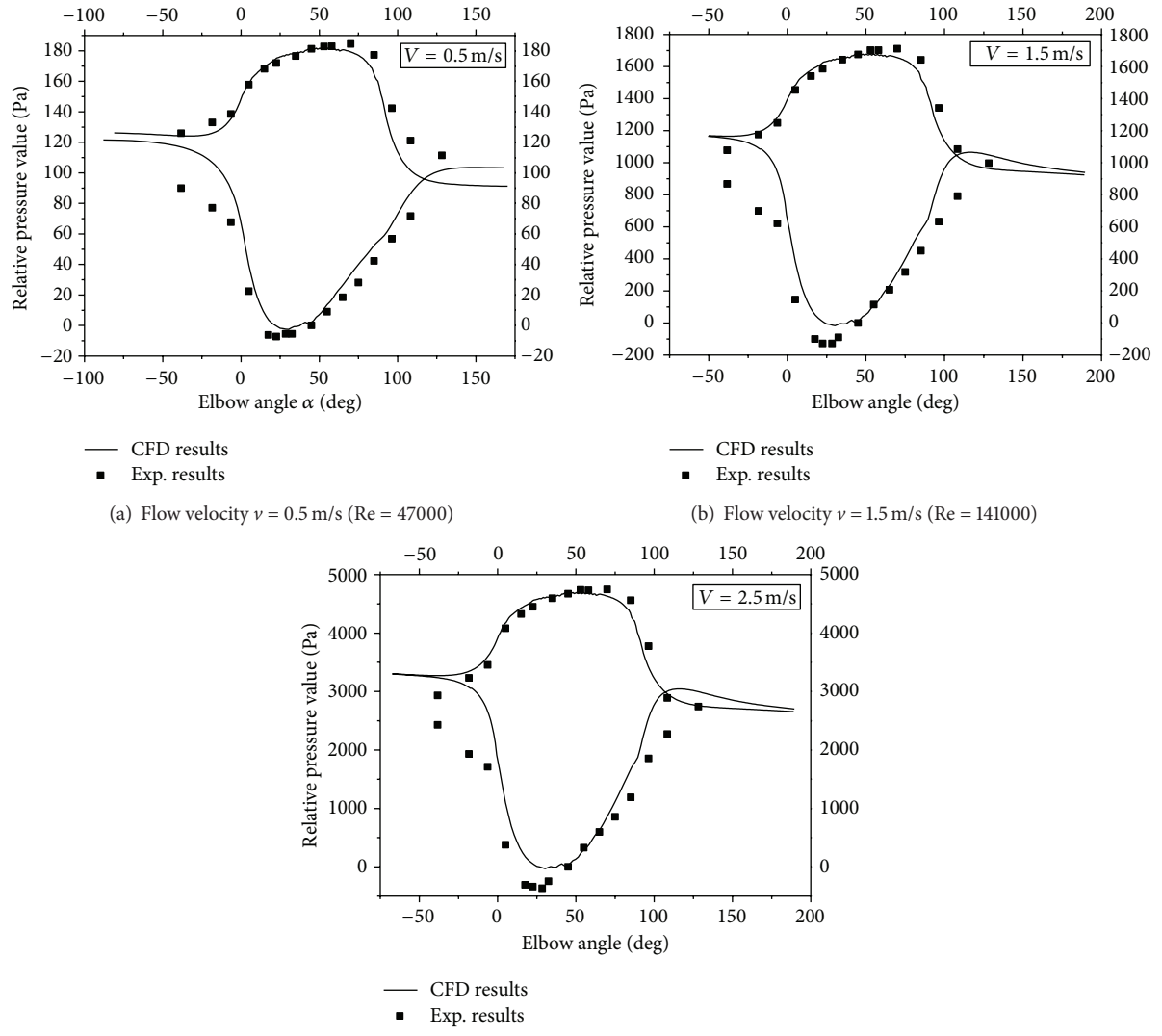

(a) Flow velocity v = 0.5 m/s (Re = 47000)

(b) Flow velocity v = 1.5 m/s (Re = 141000)

(c) Flow velocity v = 2.5 m/s (Re = 235000)

Figure 4: Comparison of the measured and predicted static pressure profile of 90° elbow.

to mark the experimental results of pressure distribution of 90° elbow and continuous curved line in the figures indicates the numerical results. Upper lines describe the pressure distribution of the outer radius wall of 90° elbow and lower lines stand for the pressure distribution of the inner radius wall zone.

In general, both measured and predicted wall static pressure distributions of 90° elbow are in satisfactory agreement for flow measurement. Figure 4 shows the quantitative comparison of the measured wall static pressure distribution of outer radius wall and inner radius wall of 90° elbow through fifteen pressure taps with the numerical simulation results at three different flow velocities. Pressure distribution is plotted against the angle between the cross section of 90° elbow and the horizontal plane. Predicted wall pressure at three flow velocity is in satisfactory agreement with measurements. Nevertheless, a few of points of inner wall before inlet of 90° elbow are overpredicted around 20–35% in comparison to the measurements. Such error can be attributed to the probable onset of transitional turbulent flow. Nevertheless, it can be noted that the predicted pressure distribution during the angle 10° ~ 80° of elbow matches the experimental

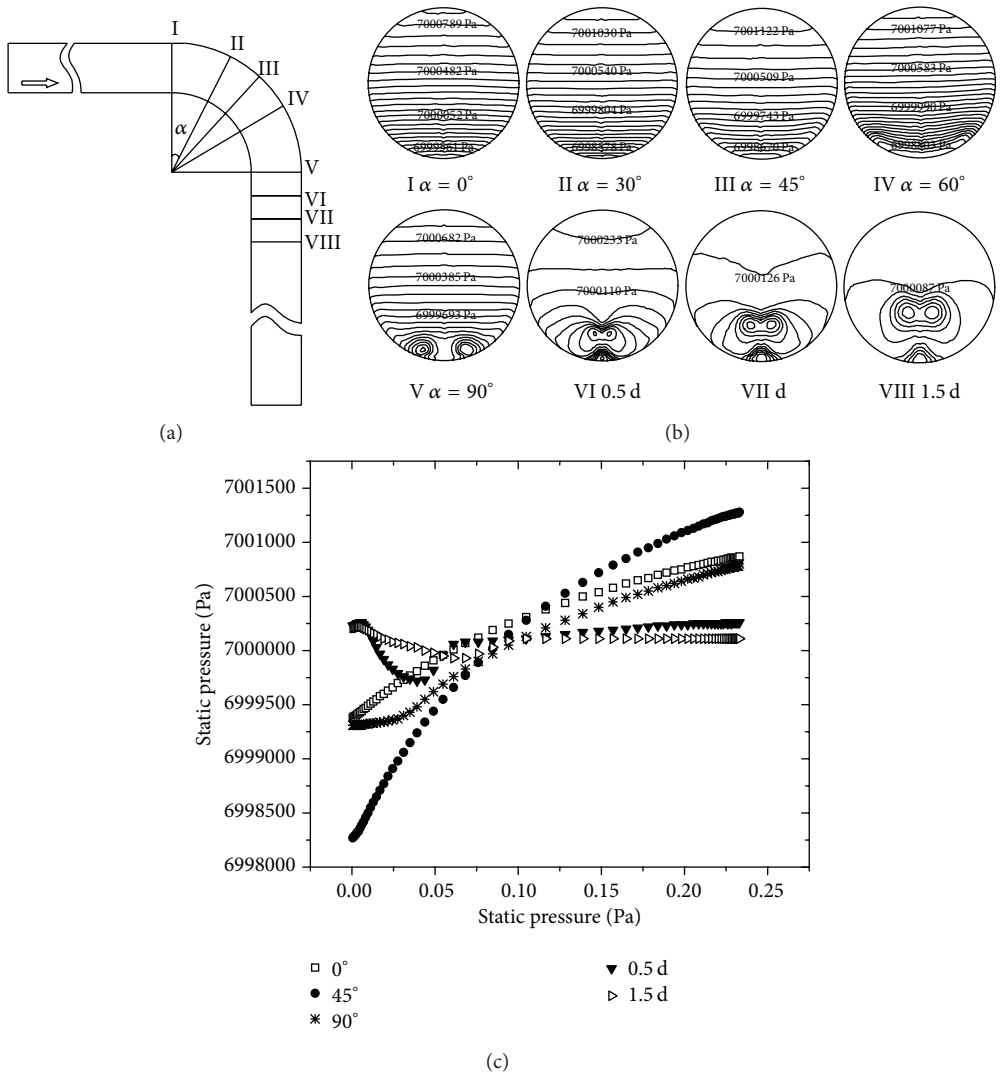

Figure 5: The typical pressure contours of 90° elbow at various pipe sections for helium gas flow under the condition 250°C and 7.0 MPa (mean velocity $v = 24.9$ m/s, Re $\approx 1.3 \times 10^6$). (a) Cross section position of a 90° elbow; (b) static pressure contours of eight cross sections; (c) static pressure distribution along the midline of 90° elbow in selected planes I, III, V, VI, and VIII.

data well. And, in practical applications, pressure measuring holes for flow measurement are normally located at 45° or 22.5° cross section of elbow. So, the numerical study is considered reasonable for the study of flow characteristics of helium gas under high temperature and high pressure for flow measurement.

4.2. Discussion of Pressure Distribution of Helium Gas Flowing through a 90° Elbow. Figure 5 presents the sectional pressure distribution of the elbow at pipe sections 0°, 30°, 45°, 60°, and 90° and additional three sections on the lower location of pipe outlet (VI, VII, and VIII). Helium gas flows through 90° elbow having the diameter $D = 233$ mm. The dimensionless curvature radius of the elbow is $R/D = 1.5$ and the length of the straight section of the pipe before the elbow is $L_e = 5D_{\text{in}}$. Figure 5(c) shows the outlines of variations of pressure in the selected cross section planes of the elbow model. It is assumed that environmental pressure P and flow velocity V of helium gas flowing the elbow is identical. One should notice that when the flow comes to the elbow, the pressure on the extrados has a rapid growth while the pressure on the intrados experiences a sharp drop under the impact of the centrifugal force resulting from the circular motion of fluid particles induced by the restriction of elbow wall when the helium gas flows through the curve structure. Figure 5(c) presents the static pressure distribution along the midline of elbow in the selected planes I, III, V, VI, and VIII.

Also, Figures 4 and 6 present the drops of the static pressure along the inner and outer radius of the elbow wall. Significant influence on the wall pressure distribution is observed and a sharp drop of inner radius wall and a rapid growth of outer wall are illustrated in Figure 6 due to the centrifugal force of helium gas. The fluid particle

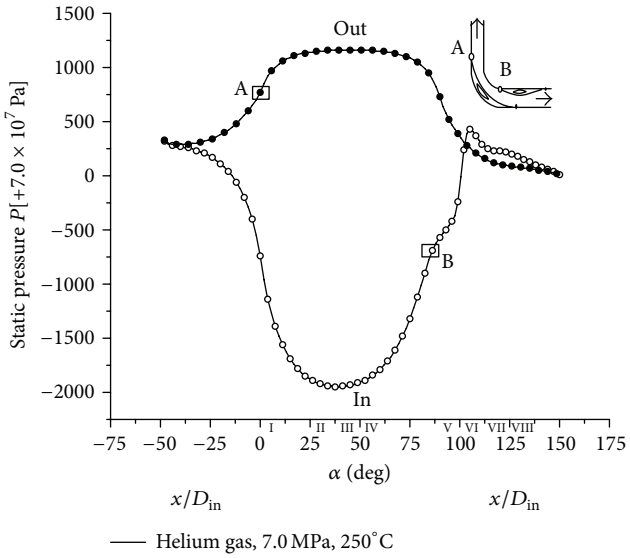

Figure 6: Changes of the static pressure along 90° elbow walls.

has a tendency of being tossed to the extrados from the intrados. When helium gas comes to the vicinity of the α = 40° cross section of 90° elbow, pressure on the extrados reaches its maximum while pressure on the intrados attains its minimum. On the extrados, this is caused by both of the centrifugal forces and the impact of the fluid on the elbow wall. On the intrados, the decline and the minimum of the pressure is induced partially by the boundary-layer separation. In the vicinity of the α = 40° cross section, the curve line representing the pressure distribution on the extrados shows a tendency of flat, which indicates that the static pressure distribution in this region is homogeneous in some sense. After this region, the pressure of the extrados begins to decline due to the reflection effect.

5. Conclusion

Numerical study of helium gas under high pressure and high temperature flowing through a 90° elbow is performed in this paper through computational fluid dynamics (CFD). Experimental study of wall static pressure distribution of 90° elbow is conducted on a self-built test system. Distribution of wall pressure is measured through 15 points located on the inner pipe wall and outer pipe wall and is used to compare with the simulation results. Investigation of helium gas under high temperature and high pressure is then carried out through the validated numerical approach. Conclusions from the simulations of helium gas flowing through 90° elbow are the following.

(1) A pressure difference is created by centrifugal force between the inside diameter and the outer side wall of 90° elbow when helium gas under high pressure and high temperature is flowing through the elbow and it is possible for flow measurement based on the pressure difference.

(2) A low level of pressure difference leads to difficulties for flow measurement and the pressure measuring hole is located on the secant of the elbow angle, that is, the angle α = 45°, in order to measure the maximum pressure difference in practical applications.

(3) On the extrados of 90° elbow, high pressure distribution is caused by the centrifugal forces and the impact of the fluid on the elbow wall. On the intrados, the decline and the minimum of pressure is induced partially by the boundary-layer separation.

Conflict of Interests

The authors declare that they have no conflict of interests regarding the publication of this paper.

Acknowledgments

The authors acknowledge the support of the National S & T Major Project of China under Grant no. ZX06901 and The Tribology Science Fund of State Key Laboratory of Tribology (Grant no. SKLTKF12B16).

References

[1] Z. Wu and H. Xiao, "Safety features of the modular HTGR," *High Technology Letters*, vol. 11, pp. 34–38, 1994.

[2] L. Zhirong, C. Liqiang, X. Xiaofei, and L. Yuan, "Inherent safety features of the modular HTGR," *Nuclear Safety*, vol. 12, no. 3, pp. 1–4, 2013.

[3] L. Yong and Z. Zuoyi, "Prospects of power conversion technology of direct-cycle helium gas turbine for MHTGR," *Nuclear Power Engineering*, vol. 20, no. 2, pp. 159–164, 1999.

[4] L. Zhiyong, L. Jun, H. Xuedong, and L. Shengqiang, "The Data measuring and acquisition system of stability experiment of steam generator for high temperature gas cooled reactor," *High Technology Letters*, vol. 01, pp. 79–81, 2002.

[5] C. Liqiang, H. Shouyin, and H. Chen, "Measuring methods for helium leakage rate of the primary coolant loop of HTR-10," *Chinese Journal of Nuclear Science and Engineering*, vol. 3, pp. 234–239, 2007.

[6] J. Barbe, F. Dijoux, C. Yardin, and T. Macé, "Measurement of helium micro flow for gas chromatography by the dilution method," *Mapan: Journal of Metrology Society of India*, vol. 27, no. 2, pp. 77–81, 2012.

[7] K. Rup and L. Malinowski, "Fluid flow identification on base of the pressure difference measured on the secant of a pipe elbow," *Forschung im Ingenieurwesen*, vol. 70, no. 4, pp. 199–206, 2006.

[8] J. C. Branch, "The effects of an upstream short radius elbow and pressure tap location on orifice discharge coefficients," *Flow Measurement and Instrumentation*, vol. 6, no. 3, pp. 157–162, 1995.

[9] K. Sudo, M. Sumida, and H. Hibara, "Experimental investigation on turbulent flow in a circular-sectioned 90-degree bend," *Experiments in Fluids*, vol. 25, no. 1, pp. 42–49, 1998.

[10] Z. J. Wang and M. J. Berger, "Towards automatic grid independent viscous solutions with an adaptive Cartesian/Quad grid flow solver," in *Fifteenth International Conference on Numerical Methods in Fluid Dynamics*, P. Kutler, J. Flores, and J.-J. Chattot, Eds., vol. 490 of *Lecture Notes in Physics*, pp. 352–357, Springer, Berlin, Germany, 1997.